# Calcium/Poly(9,9-dioctylfluorene) Interaction: A Theoretical Study

**S. L. Sun, C. S. Lin, R. Q. Zhang,* C. S. Lee, and S. T. Lee**

*Center of Super-Diamond and Advanced Films (COSDAF) & Department of Physics and Materials Science, City University of Hong Kong, Hong Kong SAR, China*

*Received: February 8, 2005; In Final Form: May 3, 2005*

The geometric and electronic structures of poly(9,9-dioctylfluorene) (PFO) oligomer interacting with Ca atoms were studied using Møller−Plesset perturbation theory. A weak interaction with little charge transfer and with a relatively long Ca−C distance (about 4.0 Å) was found when only one Ca atom was attached to a PFO unit. However, when two Ca atoms were adsorbed at a PFO unit, a strong interaction with a shorter Ca−C distance (about 2.67 Å) took place with considerable charge transfer from the Ca atom to the PFO, resulting in significant deformation in the backbone of the PFO oligomer. In the latter case, the frontier orbitals of the PFO were modified. However, the deformed PFO and its modified frontier orbitals could be recovered when oxygen was added, which is in good agreement with experimental observation.

## 1. Introduction

Organic electroluminescent (EL) devices have been actively studied in recent years since Tang and VanSlyke first demonstrated a double-layer organic light-emitting diode (OLED).[1,2] The OLED has the advantages of wide-visible-region light emission that can be used in flat-panel displays, as light sources for optical signal circuits, and other applications. Furthermore, polymer-based light-emitting diodes (PLEDs), reported by Burroughes et al. in 1990,[3] have also aroused much interest because of their promising applications. A series of recent breakthroughs in processing and applying conjugated polymer have stimulated new excitement in the field.[4−7] Poly(*p*-phenylenevinylene) (PPV) or its derivates have been dominantly used as the active light-emitting layer in PLEDs.[8] PPV-based LEDs have many advantages such as ease of fabrication, good chemical tunability to emit light from red to blue, and large, flexible emitting areas.[9−13]

Recently, however, luminescence efficiency as high as 22l m/W in PLEDs has been achieved in devices using another polymer, polyfluorene, as the active light-emitting layer.[14] Consequently, poly(9,9-dioctylfluorene) (PFO) is now attracting much interest due to the feasibility of using it to fabricate PLEDs with a low turn-on voltage, high brightness, and high efficiency.[15−19]

It is well-known that the nature of the interface between the metal electrode and the active light-emitting polymer[20] is one of the most important factors in determining PLEDs' performance.[21] In particular, the electroluminescent efficiency and turn-on voltage of OLEDs based on small molecules and polymers are greatly affected by the contact electrode which forms an injection barrier with the organic layer.[22,23] Therefore, numerous research groups have studied the interface of PLEDs.

In PFO-based devices,[24−26] Ca is widely used as a cathode because of its low work function which means it can more efficiently inject electrons into the PFO emissive layer. Experimentally, the appearance of two gap states and the vanishing of the lowest unoccupied molecular orbital (LUMO) have been observed after depositing Ca material onto PFO polymer. To better understand this phenomenon and improve the charge injection properties of the Ca/PFO interface, theoretical studies on the Ca/PFO interaction, the origin of new electronic states, and the charge transfer and dipole at the interface are needed.

In this work, a theoretical study of the geometric and electronic structures of complexes formed by PFO and low work function Ca by first-principles calculations using second-order Møller−Plesset perturbation theory (MP2) was performed. The geometric and electronic structures of complexes between PFO and Ca were revealed by studying their different interactions. Rational interpretations of recent experiments were attempted on the basis of our theoretical calculations.

## 2. Theoretical Approaches

In this work, one of our aims was to extract information about Ca/PFO interactions. Therefore, different models of Ca/PFO interaction systems were designed and subjected to investigation with different theoretical methods, including Hartree−Fock (HF) theory, density functional theory (DFT),[27−29] and MP2[30,31] using the Gaussian 98 package.[32] As these approaches, in particular the MP2 method, were impractical for studying the real Ca/PFO interaction systems with large basis sets, we needed to adopt medium-size basis sets such as 6-31G[33] and 6-31G*[34] (split valence plus *d* polarization function) for different atoms based on their different properties in the systems under consideration, following an economic scheme for basis set selection demonstrated in some of our previous work.[35] This economic basis set, in which different atoms used different basis sets, was designated as 6-31G# in this work. The economic basis set reduced considerably the CPU time. Meanwhile, the geometrical parameters and distributions of the density of states (DOS) obtained from these two approaches were found to be very close. In the study of Ca/PFO interaction reported here, we adopted 6-31G basis set for nonmetal elements (C and H) and 6-31G* for the metal atom Ca. Tests showed that this economic basis set scheme was sufficient for describing the structural and energetic features of considered systems. Moreover, to estimate the atomic charge, a natural population analysis was performed.

* Corresponding author. E-mail: aprqz@cityu.edu.hk.

10.1021/jp050677e CCC: $30.25 
Published on Web 06/14/2005

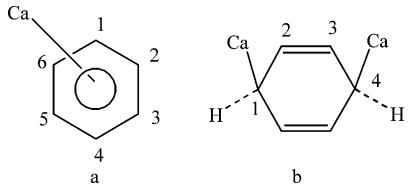


**Figure 1.** Model structures of (a) the Ca/benzene and (b) the $Ca_2$/benzene.

**TABLE 1: Geometric and Energetic Results of Ca/Benzene (Model a) Calculated with the MP2, B3LYP, and HF Methods Using a 6-31G# Basis Set (Bond Lengths in Å, Angles in deg, Energies in eV, and Charges in au)**

| | MP2 | B3LYP | HF |
|---|---|---|---|
| Ca−C1 | 3.874 | 3.785 | 5.792 |
| C1−C2−C3−C4 | 0.0 | 0.0 | 0.0 |
| binding energy | 0.378 | 0.034 | 0.005 |
| charge of Ca | −0.002 | 0.0 | 0.0 |

## 3. Results and Discussion

**3.1. Interaction between Ca and a Benzene Ring.** It is well-known that there is a strong interaction between Al atoms and conjugated polymers that form the Al−C covalent bond.[36] However, a significant interaction fails to occur when one Ca atom reacts with smaller conjugated systems.[36] For further verifications, we designed two models formed by Ca and benzene for calculations using different methods (HF, B3LYP, and MP2) at the 6-31G# level. Model a involves one Ca atom, and model b includes two Ca atoms (see Figure 1). First, model a was optimized with the above three methods; the results are summarized in Table 1. It can be seen that the distance between Ca and C is large (>3.7 Å), as predicted by all three methods. The benzene ring maintained its original planar structure due to its weak interaction with Ca and the small charge transferred from the Ca atom. The results also show that the binding energies obtained by B3LYP and HF are nearly zero. However, MP2 gave a higher binding energy, which indicates that the electron correlation effect is important in investigating the long distance interaction between metal and conjugated systems. In fact, MP2 has generally been regarded as a practical method that could reliably describe a system involving weak interaction, as we recently demonstrated using a Ca atom interacting with aromatic hydrocarbons.[37] Thus, in this work, all of the following results were calculated at the MP2/6-31G# level of theory. Comparing the projected density of states (PDOS) and the total density of states (TDOS) of the pristine benzene ring and the benzene ring after introduction of Ca, it is shown that one Ca atom does not influence the DOS of the benzene ring. Thus, the weak interaction occurs in model a with one Ca atom.

For model b, that is, the $Ca_2$/benzene system (Figure 1b), the full optimization of the geometrical structure was carried out only with the MP2/6-31G# level of theory. The bond C−Ca was found to be about 2.652 Å, and the electron transfer from each Ca to the benzene ring is about 0.526 electrons. Some geometric parameters are summarized in Table 2. These data indicate that a strong interaction occurred in Figure 1b with two Ca atoms. Moreover, the benzene ring was found to be deformed with a dihedral angle (C1−C2−C3−C4) of about 40°, as shown in Figure 1b. Although the small conjugated system may be too small to accommodate two extra electrons transferred from a Ca atom, as pointed out by Fredriksson et al.,[36] our calculation results indicate obvious charge transfer when two Ca atoms react with a benzene ring. The charge transfer is due to the deformation of the conjugated structure, which breaks down the protection provided by the $\pi$ electrons ($sp^2$ hybridization) from the attack by external atoms. The interaction between one Ca atom and the benzene ring is weak, because the benzene ring is too rigid to deform its planar structure in order to accumulate the joined electrons. However, a strong interaction occurs when two Ca atoms are added into the benzene ring. In the $Ca_2$/benzene case, the interaction between the two Ca atoms and the benzene is strong enough to deform the planar structure of benzene. Meanwhile, the loss of the planar structure causes the loss of the $\pi$-conjugated electronic structure and allows the charge transfer from the Ca atom to the benzene ring. The benzene electronic structure evolves from an $sp^2$-hybridized configuration to an $sp^3$-hybridized configuration. Hence, the original conjugated structure was broken. The changed electronic structure facilitates the charge transferring from Ca to C.

**TABLE 2: Geometric Parameters of $Ca_2$/Benzene (Model b) and Benzene with the MP2/6-31G# Method (Bond Lengths in Å, Angles in deg, and Charges in au)**

| | benzene | $Ca_2$/benzene |
|---|---|---|
| C2−C3 distance | 1.397 | 1.560 |
| C1−Ca distance | | 2.652 |
| dihedral angle C1−C2−C3−C4 | 0.0 | 40.0 |
| Ca−Ca distance | | 3.463 |
| charge at Ca | | 0.526 |

The benzene ring deformation can also be understood as follows. When two Ca atoms approach a benzene ring from a far distance, the energy of the whole system increases gradually while the benzene remains planar. However, when the two Ca atoms overcome a certain energy barrier and reach a position about 3.0 Å apart from the benzene, the net interaction between them is an attraction which leads the Ca atoms to move to their final optimized positions. The aromatic benzene tends to more easily accept four additional electrons rather than two, since it still obeys the "$4n + 2$ rule".[38,39] However, the resulting system containing ten $\pi$ electrons is not stable and easy to perform Jahn-Teller distortion which leads the benzene losing its planar structure along with a charge redistribution. Table 2 shows a Ca−Ca bond with a length of 3.463 Å. The natural population analysis shows that the two Ca atoms adopted sp-type hybridization and bonded together with a single Ca−Ca bond. This electronic structure feature explains why a benzene ring can be deformed by two attacking Ca atoms but remains planar with a single Ca atom. A related study done by Majumder et al. on a benzene attached with a $Pt_2$ molecule showed that a similar $C_{2v}$ structure to $Ca_2$/benzene shown in Figure 1b is the local minimum on the energy surface.[40]

**3.2. Interaction between Ca and PFO.** As the conjugation range of PFO is much larger than that of a benzene ring, it is of interest to determine whether there would be a stronger interaction between a Ca atom and a PFO molecule. This is studied in this section by first considering a basic repeating unit of PFO which contains 69 atoms (Figure 2a). The side alkyl chain ($C_8H_{17}$) is so large that it requires a lot of computational time for its structural optimization. However, it is expected not to contribute too much to the interaction between Ca and PFO. To study the effects of the side chains, the DOSs of PFO with two $C_8H_{17}$ chains and with the $C_8H_{17}$ chains replaced by two H atoms (Figure 2b) were calculated. Particular attention has been paid to the differences in HOMOs and LUMOs of the two structures, as they are important in determining the reactivity and charge transfer when the PFO interacts with a foreign atom, species, or compound. The study indicates that the two DOSs are nearly identical and the main contribution to the HOMOs and LUMOs is from the backbone of PFO. Because of the little contribution to the HOMOs and LUMOs from the two side

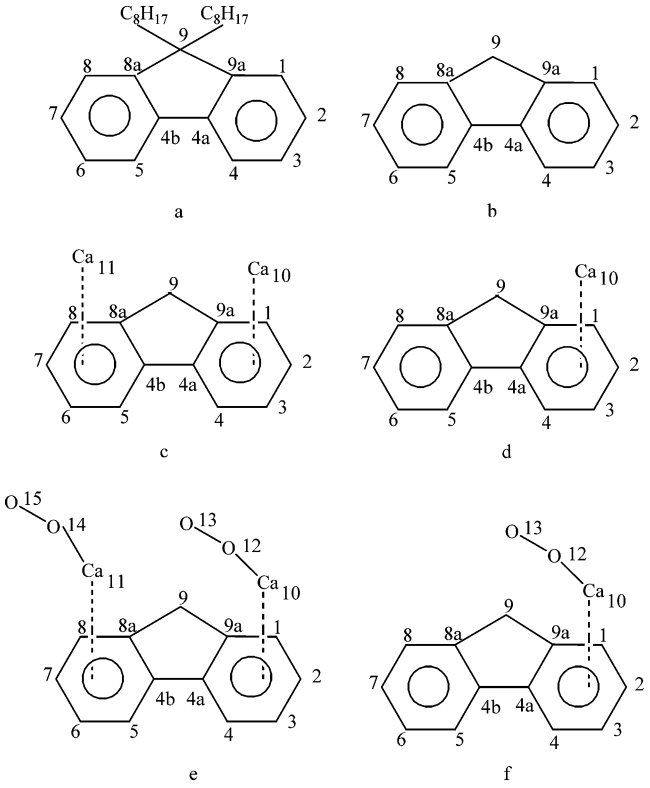


**Figure 2.** Model structures of (a) the PFO with $C_8H_{17}$, (b) the PFO with $C_8H_{17}$ replaced by H, (c) the $Ca_2$/PFO, (d) the Ca/PFO, (e) the $O_4/Ca_2$/PFO, and (f) the $O_2$/Ca/PFO. In parts b−f, the side alkyl chain $C_8H_{17}$ of PFO is replaced by an H atom.

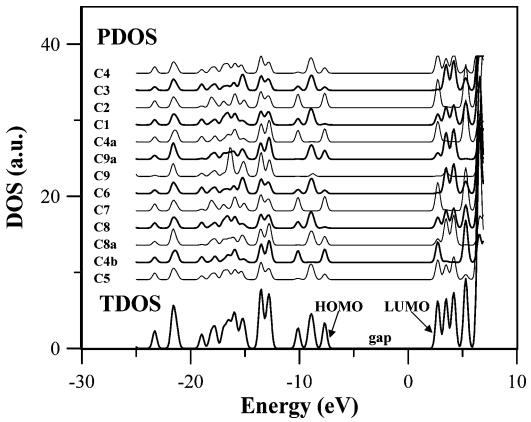


**Figure 3.** Density of states (DOS) of the PFO with $C_8H_{17}$ (see Figure 2a).

chains of $C_8H_{17}$ and the H atoms, only the DOSs from C atoms are plotted in Figure 3. Moreover, the two TDOSs (only C atoms) were presented in Figure 4a and b in order to compare them with the following calculations. To simplify the calculations, each side chain $C_8H_{17}$ of PFO is replaced by an H atom in the following calculations.

Taking the DOS of PFO into account, the main contribution to the HOMO and LUMO comes from the backbone C atoms except the atom C9 (see Figure 3). A high possibility of interaction between Ca and PFO may be expected to take place at these backbone C atoms. A Ca atom was therefore placed at every possible location on the main backbone of the PFO. Our theoretical calculations indicate that only weak interactions occur in all the complexes composed of one Ca atom and the PFO (Ca/PFO). The distance between Ca and C is about 4 Å, and the Ca atom shows a slightly negative charge in these complexes. The PFO maintains its planar structure. Moreover,

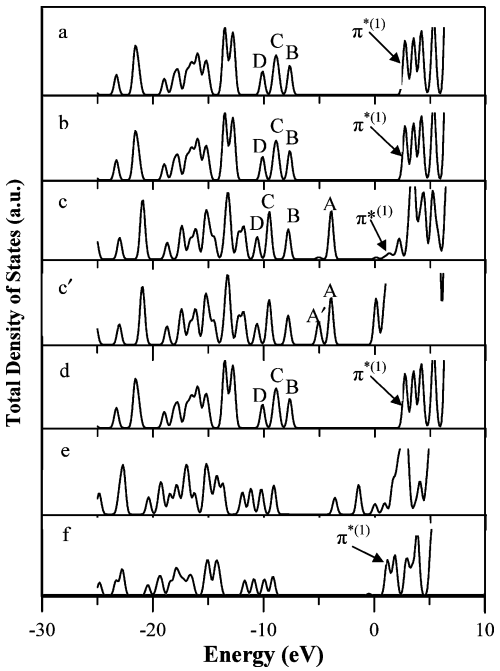


**Figure 4.** Total density of states (TDOS) including the contribution from carbon atoms only (except for c′) of (a) the PFO with $C_8H_{17}$ (see Figure 2a), (b) the PFO with $C_8H_{17}$ replaced by H (see Figure 2b), (c) the $Ca_2$/PFO (see Figure 2c), (c′) the $Ca_2$/PFO including the contribution from all atoms (see Figure 2c), (d) the Ca/PFO (see Figure 2d), (e) the $O_4/Ca_2$/PFO (see Figure 2e), and (f) the $O_2$/Ca/PFO (see Figure 2f).

the PDOS and TDOS of the PFO attached with one Ca atom are not changed compared with those of pristine PFO. This situation is similar to the result obtained in the Ca/benzene system.

On the basis of the conclusion drawn from the complex composed of two Ca atoms and a benzene ring, we also considered introducing two Ca atoms into PFO. The corresponding model $Ca_2$/PFO is shown in Figure 2c. The full geometric optimizations of the pristine PFO (Figure 2b) and $Ca_2$/PFO (Figure 2c) were carried out; some parameters of these two models are summarized in Table 3. The analysis of their bond lengths revealed that the bonds C4b−C5, C4b−C8a, C6−C7, and C7−C8 in $Ca_2$/PFO are longer than those in the pristine PFO. However, the bonds C8−C8a, C5−C6, and C4a−C4b in $Ca_2$/PFO are shorter than those in pristine PFO. The geometrical structure changes can be explained by analyzing the HOMO distributions (see Figure 5) of these two models. After adding two Ca atoms into the PFO, the electron cloud distribution of the HOMO was rearranged. In the HOMO of half of the pristine PFO, the electron cloud concentrates on two regions: one located at C4b, C5, and C8a, forming a conjugated region by the three atoms, and another located at C6, C7, and C8, forming the second conjugated region. However, according to the HOMO distribution of $Ca_2$/PFO, the conjugated structure is broken by introducing two Ca atoms. The electron cloud is rearranged to concentrate on the bonds C8−C8a, C5−C6, and C4a−C4b. Hence, these three bonds have the character of a double bond. As a result, the C8−C8a, C5−C6, and C4a−C4b bonds in $Ca_2$/PFO are shorter than the original bond lengths in the pristine PFO. The electron cloud densities of C4b−C5, C4b−C8a, C6−C7, and C7−C8 decrease, so their bond lengths are larger than their original bond lengths in pristine PFO. Moreover, the HOMO of PFO attached with two Ca atoms is almost identical to the original LUMO of pristine PFO (see Figure 5). A similar observation has been reported for an $Alq_3$ and that doped with a potassium atom.[41] Although the introduction of two Ca atoms

**TABLE 3: Geometric Parameters and Charge Distribution at Atoms of PFO (Model b) and $Ca_2$/PFO (Model c) Determined with the MP2/6-31G# Method (Bond Lengths in Å, Angles in deg, and Charges in au)**

| | | PFO | $Ca_2$/PFO |
|---|---|---|---|
| bond lengths | C4a−C4b | 1.483 | 1.415 |
| | C4b−C5 | 1.412 | 1.468 |
| | C4b−C8a | 1.426 | 1.488 |
| | C5−C6 | 1.413 | 1.406 |
| | C6−C7 | 1.416 | 1.464 |
| | C7−C8 | 1.415 | 1.462 |
| | C8−C8a | 1.406 | 1.377 |
| | Ca10−C2 | | 2.667 |
| | Ca11−C7 | | 2.668 |
| dihedral angles | C5−C4b−C8a−C8 | 0.0 | 11.8 |
| | C4b−C8a−C8−C7 | 0.0 | −0.4 |
| | C8a−C8−C7−C6 | 0.0 | −13.6 |
| | C8−C7−C6−C5 | 0.0 | 17.0 |
| | C7−C6−C5−C4b | 0.0 | −5.9 |
| | C6−C5−C4b−C8a | 0.0 | −8.5 |
| | C5−C4b−C8a−C9 | 0.0 | −168.8 |
| | C8a−C9−C9a−C4a | 0.0 | 18.4 |
| | C9−C9a−C4a−C4b | 0.0 | −12.1 |
| | C9a−C1−C2−C3 | 0.0 | 13.7 |
| | C1−C2−C3−C4 | 0.0 | −17.1 |
| | C2−C3−C4−C4a | 0.0 | 5.8 |
| | C3−C4−C4a−C9a | 0.0 | 8.8 |
| | Ca11−C7−C8−C8a | | 60.5 |
| | Ca10−C2−C1−C4a | | −61.5 |
| net charges | C1 | −0.238 | −0.288 |
| | C2 | −0.241 | −0.659 |
| | C3 | −0.245 | −0.229 |
| | C4 | −0.222 | −0.448 |
| | C4a | −0.050 | −0.191 |
| | C4b | −0.050 | −0.189 |
| | C5 | −0.222 | −0.448 |
| | C6 | −0.245 | −0.229 |
| | C7 | −0.241 | −0.658 |
| | C8 | −0.238 | −0.287 |
| | C8a | −0.009 | −0.122 |
| | C9 | −0.482 | −0.465 |
| | C9a | −0.009 | −0.121 |
| | Ca10 | | 0.927 |
| | Ca11 | | 0.926 |

has little influence on the bond angles of PFO, the dihedral angles have been changed considerably. The original planar structure is distorted into a structure with a dihedral angle (C8a−C9−C9a−C4a) of about 18°. The structure at C4b, C5, and C8a is more rigid, which helps to prevent C atoms from changing from $sp^2$ hybridization to $sp^3$ hybridization. Hence, when the Ca atoms approach the PFO, the C6−C7−C8 region would be deformed first and forms bond with one of the Ca atoms. As a result, the shortest distance is observed between the Ca10 and C2 (2.667 Å).

We further removed the Ca atom at the left side (Ca11) from the optimized model depicted in Figure 2c and obtained the model shown in Figure 2d in which the deformation of PFO was still maintained. The further geometric optimization of Figure 2d was carried out at the same level of theory. The calculation shows that the planar structure was recovered gradually during the optimization process. The Ca atom from the right-hand side was pushed away from the PFO and stabilized at a Ca−C distance of about 3.8 Å, indicating that the strong interaction between the Ca atom and the PFO has been lost. This feature further testifies that when the strong interaction occurs, the model (see Figure 2c) with two Ca atoms is more reasonable. The TDOS (only C atoms) depicted in Figure 4d is almost the same as that of pristine PFO (Figure 4b). To summarize, only the introduction of more than one Ca atom may induce a strong interaction between the Ca atom and the PFO, by changing both the geometrical structure and the electronic structure of PFO. As the number of Ca atoms deposited in the experiment was large, the strong interactions between Ca and PFO would take place and be observable.

The natural population analysis of the short Ca−C bond shows that nearly two electrons of the two Ca atoms are transferred to the PFO. The distribution of charges in the PFO with two Ca atoms shows that C2 and C7 receive about 0.4 electrons, respectively. Thus, a strong polar character exists in the bonds of Ca10−C2 and Ca11−C7, which is a feature common to the carbon−metal bond of many organometallic compounds.[42] The population of Ca11−C7 is found to be only 0.096, which verifies that Ca11−C7 is not covalent but ionic in character.

The interaction between Ca and PFO has recently been studied experimentally,[26] and a more detailed explanation of the interface formation between Ca and PFO warrants further research. In this connection, the above discussion has provided the necessary complementary knowledge. Specifically, the experimental results[26] observed by photoelectron spectroscopy (XPS and UPS) for the electronic structure evolution of PFO as Ca atoms deposited on its surface could be compared with the TDOSs of the pristine PFO and the PFO with two Ca atoms calculated in this work. In Figure 4, the TDOSs only include the sum of PDOS of the selected C atoms except for Figure 4c′. Due to the strong interaction between two Ca atoms and the PFO, the TDOS of PFO with two Ca atoms (see Figure 4c) is different from the TDOS of the pristine PFO (see Figure 4b). For $Ca_2$/PFO, the gap state A (the new HOMO) is visible in the energy gap, with the whole spectrum shifted a little to the low energy region compared to that of PFO. Moreover, the TDOS of all atoms including carbon, hydrogen, and calcium in Figure 4c′ indicates that two gap states were observable. According to the PDOS of all atoms of $Ca_2$/PFO, the gap state A on the right is due to the deformation of PFO and the gap state A′ on the left is mainly from the Ca atoms. It is noted that two gap states were also observed in a Ca doped PPV system.[43] Here, the calculated TDOS peaks of $Ca_2$/PFO in Figure 4c (C only) of unoccupied orbitals compare well with the XPS peaks of PFO as Ca atoms are deposited on its surface. Figure 4c showed that the intensity of the $\pi^{*(1)}$ level (LUMO) decreased significantly. Note that the $\pi^{*(1)}$ level (LUMO) in the experiment[26] disappeared with the deposition of Ca atoms, because of the strong interaction between Ca and PFO. The good agreement about the modifications to unoccupied orbitals and the existence of gap states in both the theoretical and experimental results indicates the capability of a theoretical approach to provide complimentary information to experiments. It also further verifies that our model with two Ca atoms (Figure 2c) is reliable.

**3.3. Oxygen Effect on the Ca and PFO Interaction.** It is interesting that the effect of Ca adsorption on PFO may be partially removed by introducing oxygen into the system.[26] To reveal the cause, the oxygen effect on the interfacial interaction and the complex formation between Ca and PFO were further investigated. A simple simulation of the reaction between a Ca atom and an oxygen molecule has been carried out. When a Ca atom meets one oxygen molecule, the distance between the two O atoms gradually increases. After passing through a transition state, the oxygen molecule becomes separated completely and CaO can be formed. On the basis of this preliminary understanding, a model, shown in Figure 2e, was designed to check the effect of oxygen on the interface between Ca and PFO. During the optimization process, the Ca11 atom was pulled far

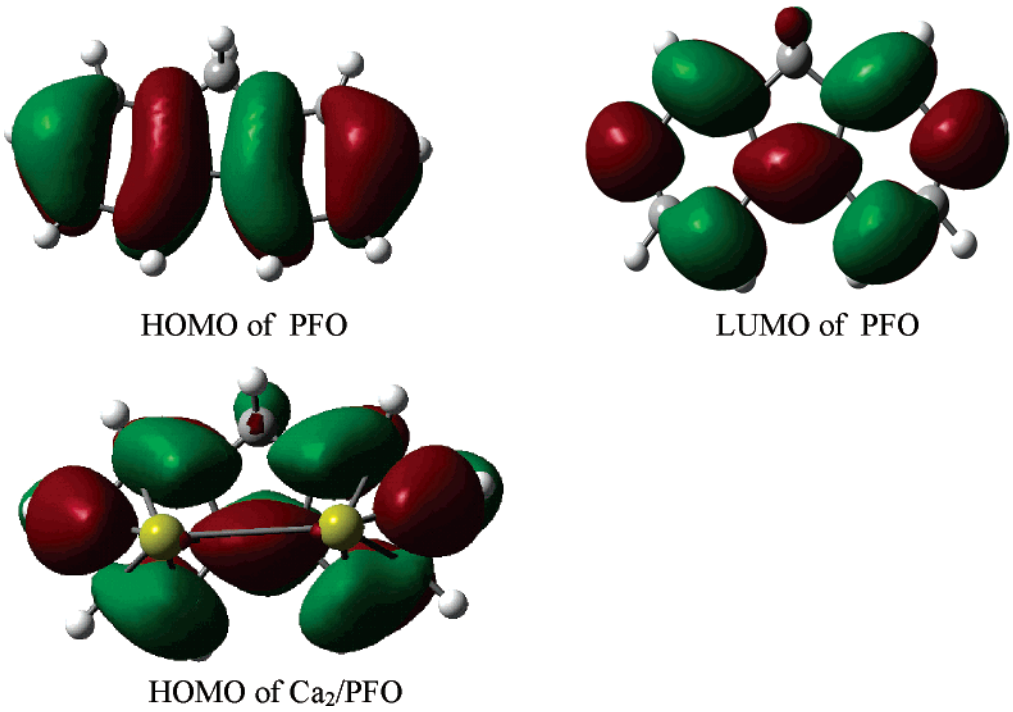


**Figure 5.** Molecular orbitals of the HOMO and LUMO of the pristine PFO and the HOMO of the $Ca_2$/PFO.

away from PFO by the O14 and O15 atoms. The TDOS was calculated and shows that the intensity of the gap state A is reduced, as depicted in Figure 4e. The change of occupied and unoccupied orbitals was observed as compared with that of $Ca_2$/PFO (Figure 4c). The previous simulations suggest that when one Ca atom moves away from the PFO, the second Ca atom cannot maintain the deformation of the PFO. Accordingly, we designed model f (see Figure 2f), in which only one Ca atom and one $O_2$ molecule were maintained. In the optimization process with Figure 2f, the Ca was also found to move away from the PFO, and the planar structure of the PFO would be recovered again. We further conducted a single point calculation of a complex of $O_2$/Ca/PFO (Figure 2f) in which the C−Ca is kept at 3.8 Å, the distance in the optimized structure shown in Figure 2d, to analyze the electronic structure changes. The calculated TDOS is shown in Figure 4f. An analysis of parts b, c, and f of Figure 4 reveals that the $\pi^{*(1)}$ level (LUMO) attenuated with the introduction of Ca atoms and it increased significantly after introducing $O_2$, showing exactly the same features of PFO before it interacts with Ca (see Figure 2b). Hence, the introduction of oxygen will recover the conjugated structure and the DOS of PFO, due to the vanishing of strong interaction. It is noted that the slight shifts of the TDOSs in Figure 4e and f to lower energy regions are due to the charge transfer from the PFO to the oxygen atoms. To summarize, the gap states emerged in the former forbidden energy gap when introducing two Ca atoms, and they were removed after introducing $O_2$. In comparison, the $\pi^{*(1)}$ level (LUMO) in the experiment[26] disappeared with the deposition of Ca atoms and it emerged again upon $O_2$ exposure. Hence, our simulation has provided an elucidation of the mechanism from the atomistic level.

## 4. Summary and Conclusions

The theoretical investigations of the interactions between Ca and conjugated systems show that a strong interaction fails to occur between one Ca atom and the conjugated PFO. However, by introducing two Ca atoms onto the PFO, a strong interaction between the Ca and the PFO takes place, in which the structure of the PFO is deformed with a dihedral angle (C8a−C9−C9a−C4a) of about 18° out-of-plane. The introduction of two Ca atoms may break the original conjugated systems of PFO. The deformed PFO molecule favors receiving the extra electrons from Ca atoms. Hence, the strong interaction between Ca and PFO is induced. Moreover, the modification of the $\pi$ and $\pi^*$ energy levels of PFO occurs due to the presence of Ca atoms, with the introduction of gap states and the attenuation of the $\pi^{*(1)}$ level (LUMO). Because an oxygen molecule may react with and take the Ca atom away from PFO, the introduction of oxygen molecules into the $Ca_2$/PFO interaction system may restore the PFO to a planar structure, eliminating the changes of the $\pi$ and $\pi^*$ levels of PFO caused by the Ca adsorption.

**Acknowledgment.** The work described in this paper is supported by grants from the Research Grants Council of the Hong Kong Special Administrative Region [Project No. CityU 2/02C], CAS-Croucher Funding Scheme for Joint Laboratories, and Chinese Academy of Sciences, China.

## References and Notes

(1) Tang, C. W.; Vanslyke, S. A. *Appl. Phys. Lett.* **1987**, *51*, 913.
(2) Tang, C. W.; Vanslyke, S. A.; Chen, C. H. *J. Appl. Phys.* **1989**, *65*, 3610.
(3) Burroughes, J. H.; Bradley, D. D. C.; Brown, A. R.; Marks, R. N.; Mackay K.; Friend, R. H.; Burns, P. L.; Holmes, A. B. *Nature* **1990**, *347*, 539.
(4) Kanatzidis, M. G. *Chem. Eng. News* **1990**, *68*, 36.
(5) Jonas, F.; Schrader, L. *Synth. Met.* **1991**, *41*, 831.
(6) Heywang, G.; Jonas, F. *Adv. Mater.* **1992**, *4*, 116.
(7) Corriu, R. J. P.; Guerin, C.; Henner B.; Kuhlmann, T.; Jean, A.; Garnier, F.; Yassar, A. *Chem. Mater.* **1990**, *2*, 351.
(8) Friend, R. H.; Gymer, R. W.; Holmes, A. B.; Burroughes, J. H.; Marks, R. N.; Taliani, C.; Bradley, D. D. C.; Dos Santos, D. A.; Bredas, J. L.; Logdlund, M.; Salaneck, W. R. *Nature* **1999**, *397*, 121.
(9) Burn, P. L.; Holmes, A. B.; Kraft, A.; Bradley, D. D. C.; Brown, A. R.; Friend, R. H.; Gymer, R. W. *Nature* **1992**, *356*, 47.
(10) Braun, D.; Heeger, A. J. *Appl. Phys. Lett.* **1991**, *58*, 1982.
(11) Braun, D.; Heeger, A. J.; Kroemer, H. *J. Electron. Mater.* **1991**, *20*, 945.

(12) Gustafsson, G.; Cao, Y.; Treacy, G. M.; Klavetter, F.; Colaneri, N.; Heeger, A. J. *Nature* **1992**, *357*, 447.
(13) Lacey, D. Presented at the 9th International Workshop on Inorganic and Organic Electro-luminesence, Bend, OR, Sept 1998; p 13.
(14) Grice, A. W.; Bradley, D. D. C.; Bernius, M. T.; Inbasekaran, M.; Wu, W. W.; Woo. E. P. *Appl. Phys. Lett.* **1998**, *73*, 629.
(15) Redecker, M.; Bradley, D. D. C.; Inbasekaran, M.; Woo, E. P. *Appl. Phys. Lett*. **1998**, *73*, 1565.
(16) Janietz, S.; Bradley, D. D. C.; Grell, M.; Giebeler, C.; Inbasekaran. M.; Woo, E. P. *Appl. Phys. Lett.* **1998**, *73*, 2453.
(17) Redecker, M.; Bradley, D. D. C.; Inbasekaran, M.; Woo. E. P. *Appl. Phys. Lett.* **1999**, *74*, 1400.
(18) Virgili, T.; Lidzey, D. G.; Bradley, D. D. C. *Adv. Mater*. **2000**, *12*, 58.
(19) Liao, L. S.; Fung, M. K.; Lee, C. S.; Lee, S. T.; Inbasekaran, M.; Woo, E. P.; Wu, W. W. *Appl. Phys. Lett*. **2000**, *76*, 3582.
(20) Salaneck, W. R.; Brédas, J. L. *Adv. Mater*. **1996**, *8*, 48.
(21) Fletcher, R. B.; Lidzey, D. G.; Bradley, D. D. C.; Walker, S.; Inbasekaran, M.; Woo, E. P. *Synth. Met.* **2000**, *111*, 151.
(22) Ishii, H.; Sugiyama, K.; Yoshimura, D.; Ito, E.; Ouchi, Y.; Seki, K. *IEEE J. Sel. Top. Quantum Electron*. **1998**, *4*, 24.
(23) Parker, I. D. *J. Appl. Phys.* **1994**, *75*, 1656.
(24) Weinfurtner, K. H.; Fujikawa, H.; Tokito, S.; Taga, Y. *Appl. Phys. Lett*. **2000**, *76*, 2502.
(25) Yu, W. L.; Cao, Y.; Pei, J. A.; Huang, W.; Heeger, A. J. *Appl. Phys. Lett*. **1999**, *75*, 3270.
(26) Liao, L. S.; Cheng, L. F.; Fung, M. K.; Lee, C. S.; Lee, S. T.; Inbasekaran, M.; Woo, E. P.; Wu, W. W. *Phys. Rev. B* **2000**, *62*, 10004.
(27) Gross, E. K. U.; Dobson, J. F.; Petersilka, M. *Top. Curr. Chem*. **1996**, *181*, 81.
(28) Curioni, A.; Andreoni, W.; Treusch, R.; Himpsel, F. J.; Haskal, E.; Seidler, P.; Heske, C.; Kakar, S.; van Buuren, T.; Terminello, L. J. *Appl. Phys. Lett*. **1998**, *72*, 1575.
(29) Curioni, A.; Boero, M.; Andreoni, W. *Chem. Phys. Lett*. **1998**, *294*, 263.
(30) Head-Gordon, M.; Pople, J. A.; Frisch, M. J. *Chem. Phys. Lett*. **1988**, *153*, 503.
(31) Frisch, M. J.; Head-Gordon, M.; Pople, J. A. *Chem. Phys. Lett*. **1990**, *166*, 275.
(32) Frisch, M. J.; Trucks, G. W.; Schlegel, H. B.; Scuseria, G. E.; Robb, M. A.; Cheeseman, J. R.; Zakrzewski, V. G.; Montgomery, J. A., Jr.; Stratmann, R. E.; Burant, J. C.; Dapprich, S.; Millam, J. M.; Daniels, A. D.; Kudin, K. N.; Strain, M. C.; Farkas, O.; Tomasi, J.; Barone, V.; Cossi, M.; Cammi, R.; Mennucci, B.; Pomelli, C.; Adamo, C.; Clifford, S.; Ochterski, J.; Petersson, G. A.; Ayala, P. Y.; Cui, Q.; Morokuma, K.; Malick, D. K.; Rabuck, A. D.; Raghavachari, K.; Foresman, J. B.; Cioslowski, J.; Ortiz, J. V.; Stefanov, B. B.; Liu, G.; Liashenko, A.; Piskorz, P.; Komaromi, I.; Gomperts, R.; Martin, R. L.; Fox, D. J.; Keith, T.; Al-Laham, M. A.; Peng, C. Y.; Nanayakkara, A.; Gonzalez, C.; Challacombe, M.; Gill, P. M. W.; Johnson, B. G.; Chen, W.; Wong, M. W.; Andres, J. L.; Head-Gordon, M.; Replogle, E. S.; Pople, J. A. *Gaussian 98*; Gaussian, Inc.: Pittsburgh, PA, 1998.
(33) Ditchfield, R.; Hehre, W. J.; Pople, J. A. *J. Chem. Phys*. **1971**, *54*, 724.
(34) Petersson, G. A.; Al-Laham, Mohammad A. *J. Chem. Phys*. **1991**, *94*, 6081.
(35) Zhang, R. Q.; Lu, W. C.; Lee, C. S.; Hung, L. S.; Lee, S. T. *J. Chem. Phys*. **2002**, *116*, 8827.
(36) Fredriksson, C.; Stafström, S. *J. Chem. Phys*. **1994**, *101*, 9137.
(37) Zhao, Y. L.; Lin, C. S.; Zhang, R. Q.; Wang, R. S. *J. Chem. Phys*., in press.
(38) Huckel, E. *Z. Phys.* **1931**, *70*, 204; **1931**, *72*, 310; **1932**, *76*, 628.
(39) Li, J.; Liu, C. W.; Lu, J. X. *THEOCHEM* **1993**, *99*, 223.
(40) Majumdar, D.; Roszak, S.; Balasubramanian, K. *J. Chem. Phys.* **2001**, *114*, 10300.
(41) Mason, M. G.; Tang, C. W.; Hung, L.-S.; Raychaudhuri, P.; Madathil, J.; Giesen, D. J.; Yan, L.; Le, Q. T.; Gao, Y.; Lee, S.-T.; Liao, L. S.; Cheng, L. F.; Salaneck, W. R.; dos Santos, D. A.; Brédas, J. L. *J. Appl. Phys.* **2001**, *89*, 2756.
(42) Eisch, J. J. *The Chemistry of Organometallic Compounds*; MacMillan: New York, 1967.
(43) Choongy, V. E.; Parky, Y.; Hsiehz, B. R.; Gao, Y. *J. Phys. D: Appl. Phys.* **1997**, *30*, 1421.